Numerical and analytical studies of critical radius in new geometries for corona discharge in air and CO_2-rich environments

Jacob A. Engle, Jeremy A. Riousset
Department of Physical Sciences, Center for Space and Atmospheric Research (CSAR), Embry-Riddle Aeronautical University, Daytona Beach, FL
(englej2@my.erau.edu)

CEDAR 2017

Abstract

In this work, we focus on plasma discharge produced between two electrodes with a high potential difference, resulting in ionization of the neutral gas particles and creating a current in the gas medium. This process, when done at low current and low temperature can create corona and "glow" discharges, which can be observed as a luminescent, or "glow," emission. The parallel plate geometry used in Paschen theory is particularly well suited to model experimental laboratory scenario. However, it is limited in its applicability to lightning rods and power lines (Moore et al., 2000). Franklin's sharp tip and Moore et al.'s rounded tip fundamentally differ in the radius of curvature of the upper end of the rod. Hence, we propose to expand the classic Cartesian geometry into spherical geometries. In a spherical case, a small radius effectively represents a sharp tip rod, while larger, centimeter-scale radius represents a rounded, or blunted tip. Experimental investigations of lightning-like discharge are limited in size. They are typically either a few meters in height, or span along the ground to allow the discharge to develop over a large distance. Yet, neither scenarios account for the change in pressure, which conditions the reduced electric field, and therefore hardly reproduce the condition of discharge as it would occur under normal atmospheric conditions (Gibson et al, 2009). In this work we explore the effects of shifting from the classical parallel plate analysis to spherical and cylindrical geometries more adapted for studies of lightning rods and power transmission lines, respectively. Utilizing Townsend's equation for corona discharge, we estimate a critical radius and minimum breakdown voltage that allows ionization of neutral gas and formation of a glow corona around an electrode in air. Additionally, we explore the influence of the gas in which the discharge develops. We use Bolsig, a numerical solver for the Boltzmann equation, to calculate Townsend coefficients for CO_2-rich atmospheric conditions (Hagelaar and Pitchford, 2005). This allows us to explore the feasibility of a glow corona on other planetary bodies such as Mars. We calculate the breakdown criterion both numerically and analytically to present simplified formulae per each geometry and gas mixture.

Objectives

- Apply Paschen theory to Cartesian, spherical, and cylindrical geometries;
- Obtain analytical expressions for critical radius and Stoletov's point;
- Develop numerical models for Cartesian, spherical, and cylindrical geometries;
- Verify numerical models and analytical solutions with experimental data;
- Establish the differences between sharp and blunt tipped rods for corona discharges
- Generalize to any atmosphere using a Boltzmann solver (Hagelaar and Pitchford, 2005).

I. Introduction

Figure 1: Glow Coronas form on the edges of a powerline transformer (Berkoff, 2005).

Corona Discharge

- Electrical discharge around a conductor due to electric field;
- Weakly ionized gas responsible for glow at visible wavelengths;
- Hypothesized to promote the formation of upward connecting leaders in lightning discharges.

Electron Avalanche

The process of electron avalanching is similar between various types of discharges:

- Initial step of a discharge;
- Release of secondary electrons in electron-neutral collision;
- Secondary electrons with enough KE to repeat the process;
- Avalanche criteria: (Raiser, 1991)

$\int_{R_1}^{R_2} \alpha_{\text{eff}}\, dr = \ln(Q) \approx$ 18-20; Q = 10^4

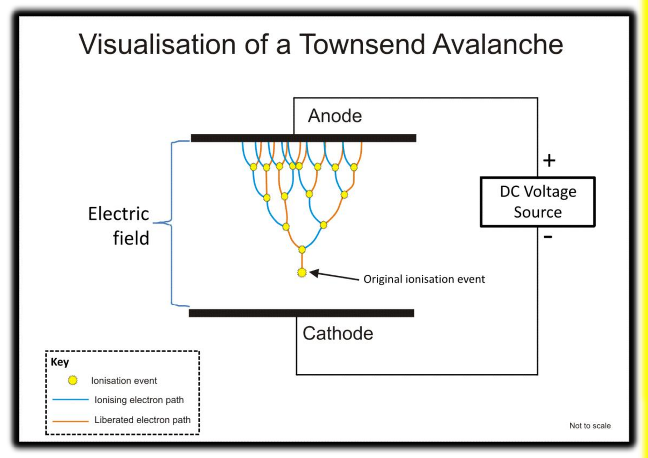

Figure 2: Visual representation of the process of an electron avalanche in Townsend's breakdown model. This can also be referred to as a Cartesian case (Gewartowski et al., 1965).

Types of Discharges

Parameter	Glow Corona	Streamer	Leader
Temperature	~300 K	~300 K	≳5000 K
Electron energy	1-2 eV	5-15 eV	1-2 eV
Electric field	0.2-2.7 kV/cm	5-7.5 kV/cm	1-5 kV/cm
Electron density	**2.6×10⁸ cm⁻³**	**5×10¹³-10¹⁵ cm⁻³**	**4×10¹⁴ cm⁻³**

Table 1: Characteristics for types of discharge at sea level in Earth's atmosphere, adapted from (Gibson et al, 2009).

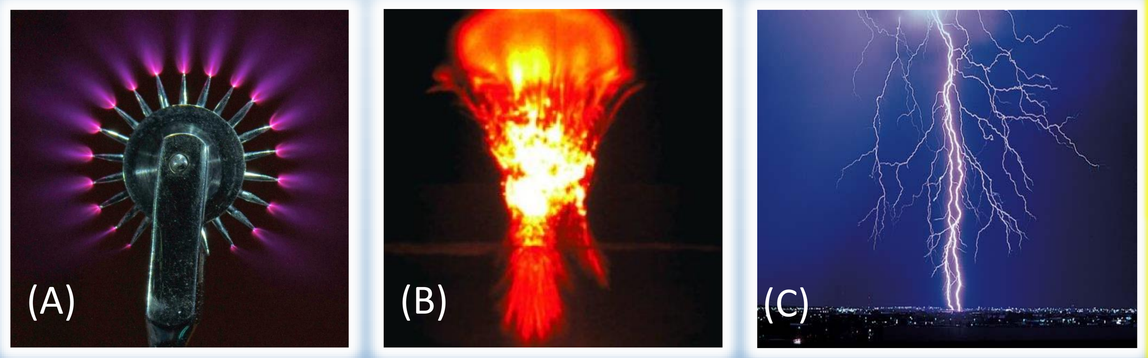

Figure 3: (A) A Wartenberg wheel with glow coronas forming at the tip of each spindle (Berkoff, 2005); (B) Streamers forming a sprite phenomenon (courtesy of H. H. C. Stenbaek-Nielsen); (C) Lightning channels as an example of leader discharge (Whetmore, 2016).

Application to Martian Studies

Motivations:

- Potential hazard due to arcing on landers and rovers;
- Interference with sensitive external systems and data measurements;
- Possibility of electrical shortage and failure.

Earth Analogy:

- Tribocharging in Martian dust storms akin to Earth sandstorms;
- Charge separation due to sedimentation & gravitation;
- Integration in the Martian global electric circuit.

Figure 4: (A) A dust storm on earth. The ionization behind this event can create lightning. (B) A dust storm photographed on the surface of Mars. The similarities with (A) indicate the possibility of dialectric breakdown on Mars. (C) The same dust storm on the surface of Mars seen from above (Yair, 2012).

II. Model Formulation

Geometry	Cartesian	Spherical	Cylindrical
Analytical	• $\int_{x_1}^{x_2} \alpha_{\text{eff}} dx = \ln(Q)$ • $x_1 = 0$ • $\alpha_{\text{eff}}(E) = Ape^{\left(\frac{-Bp}{E}\right)}$ • $d = x_2 - x_1$ • $\frac{\partial V}{\partial d} = 0$: Stoletov's point	• $\int_{R_1}^{R_2} \alpha_{\text{eff}} dr = \ln(Q)$ • $R_2 \to c$; $V(R_2) = 0$ • V(c) = 0; • $\alpha_{\text{eff}}(E) = Ape^{\left(\frac{-Bp}{E}\right)}$ • $\frac{\partial V}{\partial R_1} = 0$: Stoletov's point • $E(R_1) = E_c \frac{c^2}{{R_1}^2}$	• $\int_{R_1}^{R_2} \alpha_{\text{eff}} dr = \ln(Q)$ • $R_2 \to c$; $V(R_2) = 0$ • V(c) = 0 • $\alpha_{\text{eff}}(E) = Ape^{\left(\frac{-Bp}{E}\right)}$ • $\frac{\partial V}{\partial R_1} = 0$: Stoletov's point • $E(R_1) = E_c \frac{c}{R1}$
Numerical	• $\int_{x_1}^{x_2} \alpha_{\text{eff}} dx = \ln(Q)$ • $x_1 = 0$ • $\alpha_{\text{eff}}(E) = \frac{\nu_i(E) - \nu_a(E)}{\mu_e(E)E}$ • $d = x_2 - x_1$ • $\frac{\partial V}{\partial d} = 0$: Stoletov's point • Boltzmann solver	• $\int_{R1}^{R2} \alpha_{\text{eff}} dr = \ln(Q)$ • $R_2 \to c$; $V(R_2) = 0$ • $\alpha_{\text{eff}}(E) = \frac{\nu_i(E) - \nu_a(E)}{\mu_e(E)E}$ • $\frac{\partial V}{\partial R_1} = 0$: Stoletov's point • Boltzmann solver • $E(R_1) = E_c \frac{c^2}{{R_1}^2}$	• $\int_{R1}^{R2} \alpha_{\text{eff}} dr = \ln(Q)$ • $R_2 \to c$; $V(R_2) = 0$ • $\alpha_{\text{eff}}(E) = \frac{\nu_i(E) - \nu_a(E)}{\mu_e(E)E}$ • $\frac{\partial V}{\partial R_1} = 0$: Stoletov's point • Boltzmann solver • $E(R_1) = E_c \frac{c}{R_1}$

Assumptions:

- $p = Nk_BT$
- $E(R_1) = E(c) = E_c \approx 30 \frac{N_0}{N}$ kV/cm (Earth)
- $\nabla . \boldsymbol{E} = \rho_0 = 0$

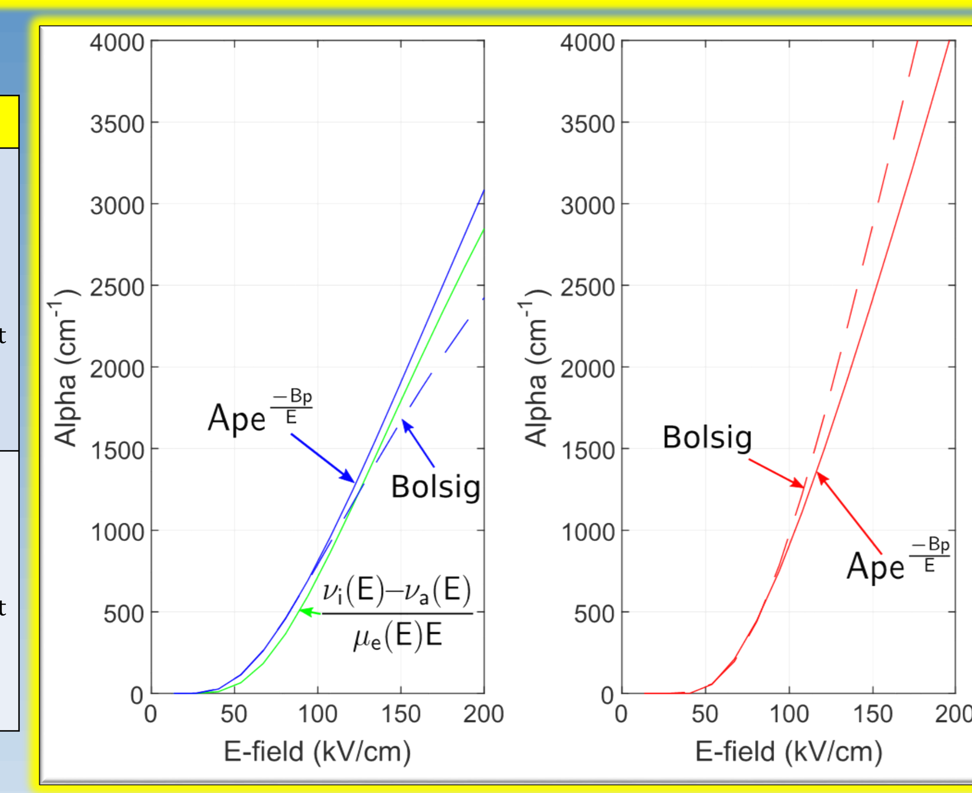

Figure 5: Fit of the exponential approximation for $\alpha_{\text{eff}}(E)$ for coefficients obtained from: Morrow and Lowke (1997), Hagelaar and Pitchford (2005).

III. Results

Cartesian solutions

- Critical electric field: $E(\text{d}) = \frac{-Bp}{\ln\left(\frac{\ln(Q)}{Apd}\right)}$
- Minimum breakdown voltage:

$$V(d) = \frac{-Bpd}{\ln\left(\frac{\ln(Q)}{Apd}\right)}$$

- Stoletov's point: $V_{\min} = \frac{eB}{A}\ln(Q)$
- CO_2 and air solutions taken at STP
- Boltzmann equation solver (Bolsig)
- Comparison with experimental data
- Convergence of solutions near Stoletov's points

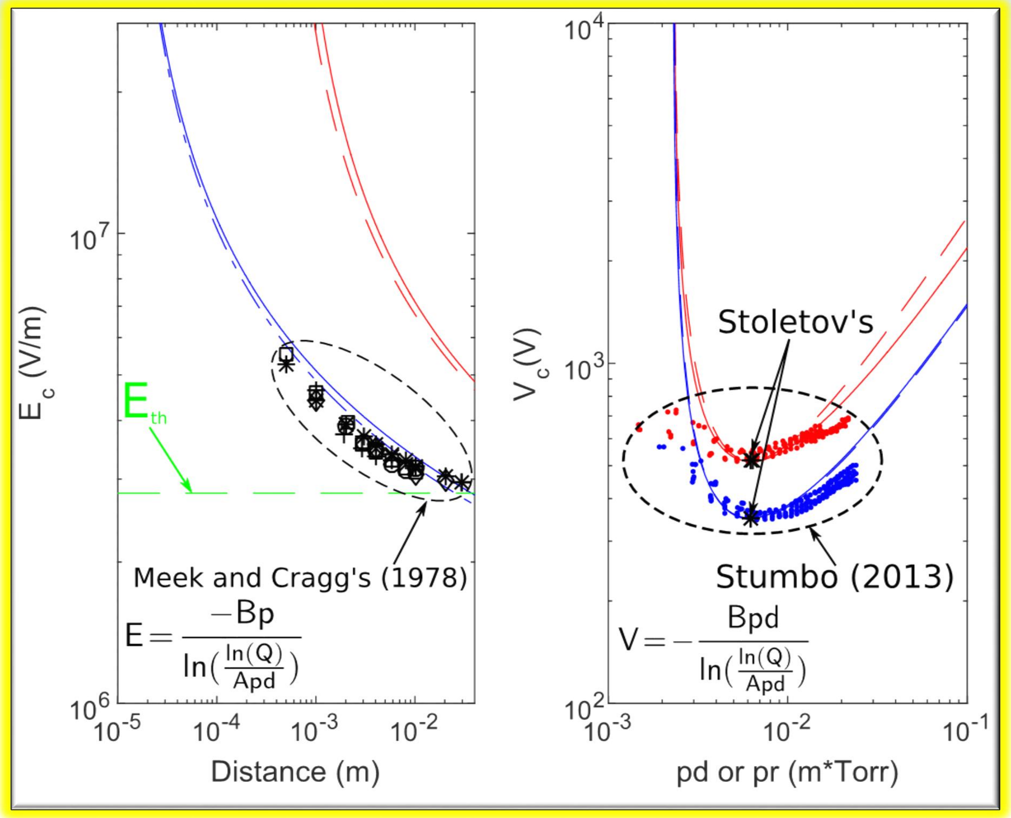

Figure 6 → : Critical electric field and breakdown voltage to meet the initiation criteria. The critical voltage curves are plotted at STP to be consistent with the conditions of the experimental data.

Spherical solutions

- Critical electric field: $E(r) = \frac{4B(\ln(Q)+Apr)^2}{\pi pA^2r^2}$
- Minimum breakdown voltage:

$$V(r) = \frac{4B(\ln(Q)+Apr)^2}{\pi pA^2 r}$$

- Stoletov's point: $V_{\min} = \frac{16B}{\pi A}\ln(Q)$.
- Largest error due to Taylor expansion of Gauss error function
- Boltzmann equation solver (Bolsig)
- Highest minimum breakdown voltage

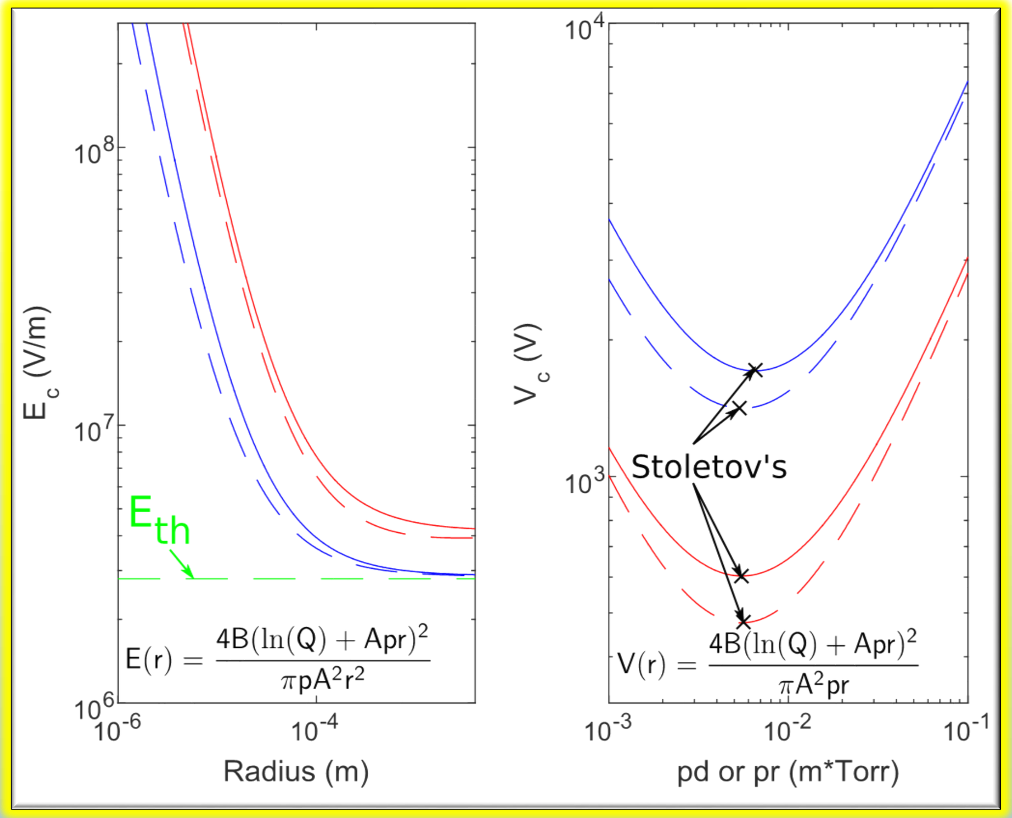

Figure 7 → : Critical electric field and breakdown voltage to meet the initiation criteria. The critical voltage curves are plotted at STP for each planetary body (Mars and Earth).

Cylindrical solutions

- Critical electric field: $E(r) = \frac{B(\ln(Q)+Apr)}{Ar\left(1-e^{\frac{-Bp}{E_0}}\right)}$
- Minimum breakdown voltage:

$$V(r) = Bpr\frac{\ln\left(\frac{B\ln(Q)}{AE_0 r}\right)}{W\left(\frac{Apr}{\ln(Q)}+1\right)}$$

- Simplification using the LambertW function
- Solutions not valid for large radii
- Boltzmann equation solver (Bolsig)

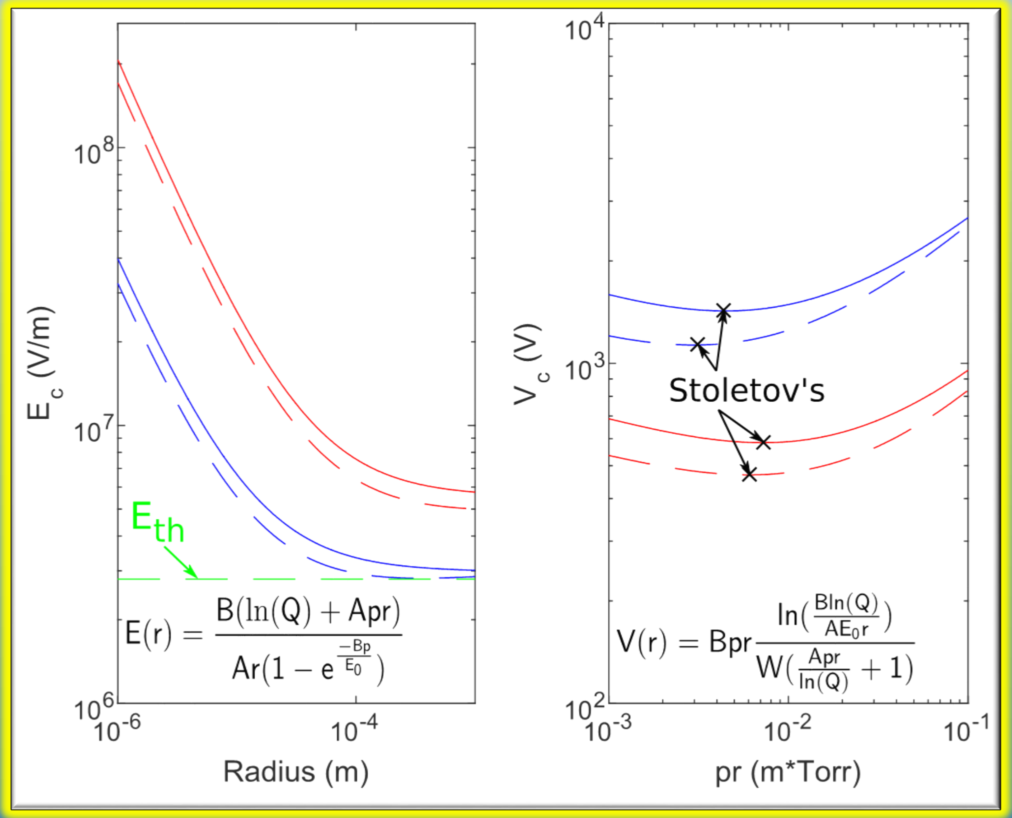

Figure 8 → : Critical electric field and breakdown voltage to meet the initiation criteria. The critical voltage curves are plotted at STP for each planetary body (Mars and Earth).

Coefficients and Stoletov's points

- A and B coefficients derived from the exponential fit accurately predict the minimum voltages (Table 2);
- Numerical, analytical, and experimental data are all in excellent agreement in the recreated Cartesian solution;
- CO_2 dominated atmospheres have a higher critical electric field than air at comparable densities;
- Mars minimum breakdown voltages are lower than Earth due to low Martian atmospheric pressure (0.6% P_{Earth}).

Coefficients	Raizer (1991) (Earth)	Morrow and Lowke (1997) (Earth)	Bolsig+ (Earth)	Bolsig+ (Mars)
A (1/cm/Torr)	15	7.7	9.29	33.44
B (V/cm/Torr)	365	274.7	295.18	430.07

Table 2: Exponential approximation coefficients (A and B) from Figure 5 found from fitting: $\alpha_{\text{eff}}(E) = Ape^{\left(\frac{-Bp}{E}\right)}$

Stoletov's Point: $V_{\min}$ (V)	Analytical	Numerical
Cartesian (Air)	348.2	350.9
Cartesian (CO_2)	517.6	603
Spherical (Earth)	1414	1709
Spherical (Mars)	475.4	603.1
Cylindrical (Earth)	1426	1132
Cylindrical (Mars)	584.3	469.8

Table 3: The minimum breakdown voltages for each geometry and atmosphere; also known as Stoletov's points.

IV. CONCLUSIONS

The results and conclusions obtained in this work can be summarized as follows:

- A new model for calculations of the critical radius and minimum breakdown voltage for Corona discharge in Cartesian, spherical, and cylindrical geometries is presented;
- The model is validated using classic Paschen theory and experimental data in air from Meek and Craggs (1978) and CO_2 from Stumbo (2013);
- We expand classic Paschen theory into an analytical solution for spherical and cylindrical geometry;
- Our numerical model and the analytical solution show excellent agreement with experimental data;
- The significantly lower pressure on Mars compared to Earth lowers the minimum breakdown voltage required to create corona discharge.

Acknowledgements:
This work is supported by the Embry-Riddle Aeronautical University Office of Undergraduate Research (ERAU) and the Center for Space and Atmospheric Research (CSAR).

REFERENCES

- E. Berkoff, *The Corona Discharge: Its Properties and Uses* - Colorado Wire & Cable (2015).
- W. M. Farrell and M. D. Desch. Is there a Martian atmospheric electric circuit? *J. Geophys. Res.*, 106:7591–7596, 4 (2001). doi: 10.1029/2000JE001271.
- J. Gewartoski, J. W. Watson, H. Alexander. Principles of Electron Tubes: Including Grid-controlled Tubes, Microwave Tubes and Gas Tubes, D. Van Nostrand Co., Inc. (1965).
- A. S. Gibson, J. A. Riousset, and V. P. Pasko. Minimum breakdown voltages for corona discharge in cylindrical and spherical geometries, NSF EE REU Penn State Annual Research Journal, 7, 1-17 (2009).
- G. J. M. Hagelaar and L. C. Pitchford. Solving the Boltzmann equation to obtain electron transport coefficients and rate coefficients for fluid models. *Plasma Sources Sci. Technol.*, 14(4):722–733, (2005).
- W. A. Lyons, CCM, T. E. Nelson, R. A. Armstrong, V. P. Pasko, and M. A. Stanley. Upward electrical discharges from thunderstorm tops. *Bull. Am. Meteorol. Soc.*, 84(4):445–454, (2003). doi: 10.1175/BAMS-84-4-445.
- J. M. Meek and J. D. Craggs. *Electrical Breakdown of Gases*. John Wiley and Sons, New York, NY, (1978).
- C. B. Moore, W. Rison, J. Mathis and G. Aulich, Lightning rod improvement studies, J. Appl. Meteor., 39 (5) 593- 609 (2000).
- R. Morrow and J. J. Lowke. Streamer propagation in air. *J. Phys. D: Appl. Phys.*, 30:614–627, (1997).
- Y. P. Raizer. *Gas Discharge Physics*. Springer-Verlag, New York, NY, (1991).
- R. Whetmore, Electrical Energy, In Compton's by Brittanica (2016).
- Y. Yair. New results on planetary lightning. *Adv. Space Res.*, 50(3):293–310, 8 (2012). doi: 10.1016/j.asr.2012.04.013.